CLEO CONF 96-11
ICHEP96 PA04-050

Study of Gluon versus Quark Fragmentation in $\Upsilon \to gg\gamma$ and $e^+e^- \to \mathrm{q\bar{q}}\gamma$ Events

CLEO Collaboration

(July 22, 1996)

Abstract

Using data collected with the CLEO II detector at the Cornell Electron Storage Ring, we have compared the charged particle multiplicities observed in $\Upsilon(1\mathrm{S}) \to gg\gamma$ to $e^+e^- \to q\bar{q}\gamma$ events. We determine a ratio for the mean charged multiplicity observed in $\Upsilon(1\mathrm{S}) \to gg\gamma$ events, $< n^{\pm}_{\mathrm{gluon}} >$, to the mean charged multiplicity observed in $e^+e^- \to q\bar{q}\gamma$ events, $< n^{\pm}_{\mathrm{quark}} >$, to be $R_{\mathrm{chrg}} \equiv \frac{<n^{\pm}_{gluon}>}{<n^{\pm}_{\mathrm{quark}}>} = 1.04 \pm 0.02(\mathrm{stat}) \pm 0.04(\mathrm{syst})$ for jet energies less than 7 GeV.

L. Gibbons,[1] S. D. Johnson,[1] Y. Kwon,[1] S. Roberts,[1] E. H. Thorndike,[1] C. P. Jessop,[2]
K. Lingel,[2] H. Marsiske,[2] M. L. Perl,[2] S. F. Schaffner,[2] D. Ugolini,[2] R. Wang,[2] X. Zhou,[2]
T. E. Coan,[3] V. Fadeyev,[3] I. Korolkov,[3] Y. Maravin,[3] I. Narsky,[3] V. Shelkov,[3]
R. Stroynowski,[3] J. Staeck,[3] I. Volobouev,[3] J. Ye,[3] M. Artuso,[4] A. Efimov,[4] M. Gao,[4]
M. Goldberg,[4] R. Greene,[4] F. Frasconi,[4] D. He,[4] S. Kopp,[4] G. C. Moneti,[4] R. Mountain,[4]
Y. Mukhin,[4] S. Schuh,[4] T. Skwarnicki,[4] S. Stone,[4] X. Xing,[4] J. Bartelt,[5] S. E. Csorna,[5]
V. Jain,[5] S. Marka,[5] A. Freyberger,[6] R. Godang,[6] D. Gibaut,[6] K. Kinoshita,[6] I. C. Lai,[6]
P. Pomianowski,[6] S. Schrenk,[6] G. Bonvicini,[7] D. Cinabro,[7] L. Perera,[7] B. Barish,[8]
M. Chadha,[8] S. Chan,[8] G. Eigen,[8] J. S. Miller,[8] C. O'Grady,[8] M. Schmidtler,[8] J. Urheim,[8]
A. J. Weinstein,[8] F. Würthwein,[8] D. M. Asner,[9] D. W. Bliss,[9] W. S. Brower,[9] G. Masek,[9]
H. P. Paar,[9] M. Sivertz,[9] J. Gronberg,[10] C. M. Korte,[10] D. J. Lange,[10] R. Kutschke,[10]
S. Menary,[10] R. J. Morrison,[10] S. Nakanishi,[10] H. N. Nelson,[10] T. K. Nelson,[10] C. Qiao,[10]
J. D. Richman,[10] D. Roberts,[10] A. Ryd,[10] H. Tajima,[10] M. S. Witherell,[10] R. Balest,[11]
B. H. Behrens,[11] K. Cho,[11] W. T. Ford,[11] H. Park,[11] P. Rankin,[11] J. Roy,[11] J. G. Smith,[11]
J. P. Alexander,[12] C. Bebek,[12] B. E. Berger,[12] K. Berkelman,[12] K. Bloom,[12] D. G. Cassel,[12]
H. A. Cho,[12] D. M. Coffman,[12] D. S. Crowcroft,[12] M. Dickson,[12] P. S. Drell,[12] R. Ehrlich,[12]
R. Elia,[12] A. D. Foland,[12] P. Gaidarev,[12] R. S. Galik,[12] B. Gittelman,[12] S. W. Gray,[12]
D. L. Hartill,[12] B. K. Heltsley,[12] P. I. Hopman,[12] S. L. Jones,[12] J. Kandaswamy,[12]
N. Katayama,[12] P. C. Kim,[12] D. L. Kreinick,[12] T. Lee,[12] Y. Liu,[12] G. S. Ludwig,[12]
J. Masui,[12] J. Mevissen,[12] N. B. Mistry,[12] C. R. Ng,[12] E. Nordberg,[12] M. Ogg,[12,1]
J. R. Patterson,[12] D. Peterson,[12] D. Riley,[12] A. Soffer,[12] C. Ward,[12] P. Avery,[13]
M. Athanas,[13] C. D. Jones,[13] M. Lohner,[13] C. Prescott,[13] S. Yang,[13] J. Yelton,[13] J. Zheng,[13]
G. Brandenburg,[14] R. A. Briere,[14] D. Y.-J. Kim,[14] T. Liu,[14] M. Saulnier,[14] R. Wilson,[14]
H. Yamamoto,[14] T. E. Browder,[15] F. Li,[15] Y. Li,[15] J. L. Rodriguez,[15] T. Bergfeld,[16]
B. I. Eisenstein,[16] J. Ernst,[16] G. E. Gladding,[16] G. D. Gollin,[16] E. Johnson,[16] I. Karliner,[16]
M. Palmer,[16] M. Selen,[16] J. J. Thaler,[16] K. W. Edwards,[17] A. Bellerive,[18] D. I. Britton,[18]
R. Janicek,[18] D. B. MacFarlane,[18] K. W. McLean,[18] P. M. Patel,[18] A. J. Sadoff,[19]
R. Ammar,[20] P. Baringer,[20] A. Bean,[20] D. Besson,[20] D. Coppage,[20] C. Darling,[20] R. Davis,[20]
N. Hancock,[20] S. Kotov,[20] I. Kravchenko,[20] N. Kwak,[20] L. J. Weinstein,[20] S. Anderson,[21]
Y. Kubota,[21] M. Lattery,[21] J. J. O'Neill,[21] S. Patton,[21] R. Poling,[21] T. Riehle,[21]
A. Smith,[21] V. Savinov,[21] M. S. Alam,[22] S. B. Athar,[22] Z. Ling,[22] A. H. Mahmood,[22]
H. Severini,[22] S. Timm,[22] F. Wappler,[22] A. Anastassov,[23] S. Blinov,[23,2] J. E. Duboscq,[23]
R. Fulton,[23] D. Fujino,[23] K. K. Gan,[23] T. Hart,[23] K. Honscheid,[23] H. Kagan,[23] R. Kass,[23]
J. Lee,[23] M. Sung,[23] A. Undrus,[23,2] R. Wanke,[23] A. Wolf,[23] M. M. Zoeller,[23] B. Nemati,[24]
S. J. Richichi,[24] W. R. Ross,[24] P. Skubic,[24] M. Wood,[24] M. Bishai,[25] J. Fast,[25] E. Gerndt,[25]
J. W. Hinson,[25] D. H. Miller,[25] E. I. Shibata,[25] I. P. J. Shipsey,[25] and M. Yurko[25]

[1]University of Rochester, Rochester, New York 14627
[2]Stanford Linear Accelerator Center, Stanford University, Stanford, California 94309
[3]Southern Methodist University, Dallas, Texas 75275

---

[1]Permanent address: University of Texas at Austin.

[2]Permanent address: BINP, RU-630090 Novosibirsk, Russia.

[4]Syracuse University, Syracuse, New York 13244
[5]Vanderbilt University, Nashville, Tennessee 37235
[6]Virginia Polytechnic Institute and State University, Blacksburg, Virginia 24061
[7]Wayne State University, Detroit, Michigan 48202
[8]California Institute of Technology, Pasadena, California 91125
[9]University of California, San Diego, La Jolla, California 92093
[10]University of California, Santa Barbara, California 93106
[11]University of Colorado, Boulder, Colorado 80309-0390
[12]Cornell University, Ithaca, New York 14853
[13]University of Florida, Gainesville, Florida 32611
[14]Harvard University, Cambridge, Massachusetts 02138
[15]University of Hawaii at Manoa, Honolulu, Hawaii 96822
[16]University of Illinois, Champaign-Urbana, Illinois 61801
[17]Carleton University, Ottawa, Ontario, Canada K1S 5B6
and the Institute of Particle Physics, Canada
[18]McGill University, Montréal, Québec, Canada H3A 2T8
and the Institute of Particle Physics, Canada
[19]Ithaca College, Ithaca, New York 14850
[20]University of Kansas, Lawrence, Kansas 66045
[21]University of Minnesota, Minneapolis, Minnesota 55455
[22]State University of New York at Albany, Albany, New York 12222
[23]Ohio State University, Columbus, Ohio 43210
[24]University of Oklahoma, Norman, Oklahoma 73019
[25]Purdue University, West Lafayette, Indiana 47907

I. INTRODUCTION

Many experiments have searched for differences between quark and gluon fragmentation [1]-[19]. At Z^0 energies, $q\bar{q}g$ events are readily distinguished by their three-jet topology. Within such events, quark and gluon jets can be separated by a variety of techniques including vertex tagging. Since gluons rarely fragment into heavy quarks, they will produce jets which vertex at the e^+e^- interaction point. Quark jets, to the contrary, tend to form a detached vertex when the jet contains a long-lived bottom or charm quark. One of the primary deficiencies of three-jet techniques is that the observed final state hadrons must be assigned to primary partons. However, the fragmentation process is not completely perturbative, and associating the primary partons with the final state hadrons relies on Monte Carlo simulations.

The 10 GeV center of mass energy range offers a unique opportunity to probe quark and gluon fragmentation effects, without relying on Monte Carlo simulation to associate the final state hadrons with an initial state parton. The decay $\Upsilon(1S) \to gg\gamma$ allows one to compare the gg system in a $gg\gamma$ event with the $q\bar{q}$ system in $e^+e^- \to q\bar{q}\gamma$ events. In both cases, the system recoiling against the photon consists (to lowest order) of hadrons which have evolved from either a two-gluon or a quark-antiquark system. The properties of the recoil systems can then be compared directly. Although, in both cases, there may be gluon radiation from the initial partons, we do not consider such radiation explicitly in this analysis.

II. DETECTOR AND DATA SAMPLE

The CLEO II detector is a general purpose solenoidal magnet spectrometer and calorimeter. Elements of the detector, as well as performance characteristics, are described in detail elsewhere [20]. The detector was designed for efficient triggering and reconstruction of two-photon, tau-pair, and hadronic events. Measurements of charged particle momenta are made with three nested coaxial drift chambers consisting of 6, 10, and 51 layers, respectively. These chambers fill the volume from r=3 cm to r=1 m, where r is the radial coordinate relative to the beam (z) axis. This system achieves a momentum resolution of $(\delta p/p)^2 = (0.0015p)^2 + (0.005)^2$, where p is the momentum, measured in GeV/c. Pulse height measurements in the main drift chamber provide specific ionization resolution of 6.5% for Bhabha events, giving good K/π separation for tracks with momenta up to 700 MeV/c. Outside the central tracking chambers are plastic scintillation counters which are used as a fast element in the trigger system and also provide particle identification information from time of flight measurements.

Beyond the time of flight system is the electromagnetic calorimeter, consisting of 7800 thallium doped CsI crystals. The central "barrel" region of the calorimeter covers about 75% of the solid angle and has an energy resolution of

$$\frac{\sigma_{\mathrm{E}}}{E}(\%) = \frac{0.35}{E^{0.75}} + 1.9 - 0.1E, \tag{1}$$

where E is the shower energy in GeV. This parameterization translates to an energy resolution of about 4% at 100 MeV and 1.2% at 5 GeV. Two end-cap regions of the crystal calorimeter extend solid angle coverage to about 95% of 4π, although energy resolution is not quite as good as that of the barrel region. The tracking system, time of flight counters, and calorimeter are all contained within a 1.5 Tesla superconducting coil. Flux return and tracking chambers used for muon detection are located immediately outside the coil and in the two end-cap regions.

We use data collected at the $\Upsilon(1S)$ resonance, with center-of-mass energy $E_{cm} = 9.46$ GeV, and from the continuum region, center-of-mass energy $E_{cm} = 10.52$ GeV, just below the $\Upsilon(4S)$ resonance. The integrated luminosities for the $gg\gamma$ data and for the $q\bar{q}\gamma$ data are 63 pb^{-1} and 198 pb^{-1}, respectively. The 9.46 GeV data provides a source of $gg\gamma$ events via $\Upsilon(1S) \to gg\gamma$; the 10.52 GeV data provides a source of $e^+e^- \to q\bar{q}\gamma$ events, where the photon results primarily from initial state radiation. We compare events where the invariant masses of the systems recoiling against the hard photon (M_{recoil}) are the same.

To suppress QED events, (e.g. $e^+e^- \to e^+e^-e^+e^-$), we require that the thrust of the event be less than 0.97, and that there be at least 3 good charged tracks in the event. Photon candidates are selected from showers with widths and patterns of energy deposition consistent with that of a photon, as opposed to other neutral hadrons (e.g. π^0's, K^0_{L}, neutrons, etc.). We require $|\cos\theta_\gamma| < 0.75$ (θ_γ is defined here as the polar angle between the beam and the direct photon), to eliminate events in which particles are lost down the beam pipe.

Four different candidate event samples are investigated:

1. $gg\gamma$ and $q\bar{q}\gamma$ samples, as defined above.

2. ggg and $q\overline{q}$ events containing a π^0 of energy comparable to the photon in the gamma-tagged sample (referred to as $gg(\pi^0)$ and $q\overline{q}(\pi^0)$ events, respectively). This allows us to quantify the effect of backgrounds from π^0 decays.

III. EXPERIMENTAL TECHNIQUE

One of the most basic parameters used to characterize any event is the mean charged track multiplicity, $< N_{chrg} >$. We plot $< N_{chrg} >$ as a function of mass recoiling against the direct photon (defined by $M_{recoil} = \sqrt{4E^2_{\text{beam}} \cdot (1 - E_\gamma/E_{\text{beam}})}$), covering the recoil mass range from 4 to 7 GeV/c^2. This mass interval corresponds to $0.45 < E_\gamma/E_{\text{beam}} < 0.82$ for the $gg\gamma$ sample. We require the recoil mass to be greater than 4 GeV/c^2 to ensure that we are above $c\bar{c}\gamma$ threshold; our $q\overline{q}$ jet sample therefore includes u,d,s,c quarks uniformly.

To select $gg\gamma$ events, we must subtract the background from $q\bar{q}\gamma$ and $e^+e^- \to \tau\tau\gamma$. By subtracting a "raw" $q\bar{q}\gamma$ sample, (which includes $\tau\tau\gamma$ events that also occur at the continuum of the $\Upsilon(4S)$ resonance), we account for all of the backgrounds to $gg\gamma$ at the $\Upsilon(1S)$ energy. The $q\bar{q}\gamma$ background comprises about 10% percent of the $\Upsilon(1S)$ direct photon sample.

Similarly, in order to isolate $q\bar{q}\gamma$ events at 9.46 GeV/c^2, we must quantify $\tau\tau\gamma$ contamination. This is done using a Monte Carlo simulation of tau pair events. We found that $\tau\tau\gamma$ events comprise about 10% of the $q\bar{q}\gamma$ data sample passing the other event selection cuts specified above. Beam gas and two photon backgrounds were investigated and found to be negligibly small.

Our backgrounds are summarized below:

Sample	Background (%)
$gg\gamma$	Sum of all non-$gg\gamma$ events (10%)
$q\bar{q}\gamma$	$\tau\tau\gamma$ (10%)
$q\bar{q}\gamma$	$\gamma\gamma$ (< 1%)
$q\bar{q}\gamma$	beam-gas (< 1%)

We therefore define our pure $gg\gamma$ (9.46 GeV/c^2) and $q\bar{q}\gamma$ (10.52 GeV/c^2) sample as follows:

- pure $gg\gamma$ = "raw" $gg\gamma$ - "raw" $q\bar{q}\gamma$ (scaled by luminosity and energy dependence of the e^+e^- cross-section)
- pure $q\bar{q}\gamma$ = "raw" $q\bar{q}\gamma$ - $\tau\tau\gamma$ (from Monte Carlo)

In order to determine the level of π^0 contamination, we determine how often a single high energy photon can be matched with other photons in the same event to form a π^0. Such photons are vetoed as likely π^0 daughters. Knowing the likelihood that the second π^0 daughter photon will go undetected, we determine the fraction of our direct photon candidates which are π^0 daughters, but are not vetoed as such (Figure 1). The likelihood of detecting the second photon varies from 44% at $M_{recoil} = 5.6$ GeV/c^2 to 77% at $M_{recoil} = 4$ GeV/c^2.

To determine how our charged multiplicity values are being influenced by our π^0 background, we make a comparison plot of the charged multiplicity distribution for $gg\gamma$ vs. $ggg(\pi^0)$ events, and a similar plot for $q\bar{q}\gamma$ vs. $q\bar{q}(\pi^0)$ events. From Figure 2, we see that the charged multiplicity distribution for $gg\gamma$ and $ggg(\pi^0)$ events are similar. We include the uncertainty due to π^0 backgrounds in the systematic error on our final ratios.

In Figure 3, we show the multiplicity distributions in bins of recoil mass for our $gg\gamma$ and $q\bar{q}\gamma$ samples. From these Figures, we extract the mean multiplicities as a function of gg or $q\bar{q}$ mass, for pure $gg\gamma$ and $q\bar{q}\gamma$ samples. As shown in Figure 4, the ratio of $< N_{chrg} >$ resulting from gluon fragmentation to $< N_{chrg} >$ from quark fragmentation is $R_{chrg} = 1.04 \pm 0.02$.

IV. SYSTEMATIC ERRORS

1. fiducial cut

We explicitly consider the dependence of the mean multiplicity on the dip angle, $|\cos\theta_\gamma|$, of the direct photon. We expect that initial state radiation $q\bar{q}\gamma$ events tend to produce photons that are more forward peaked (have larger values of $|\cos\theta_\gamma|$) than for $gg\gamma$. For $q\bar{q}\gamma$ events, we therefore expect that the particles emerging on the other side of the event, opposite the high energy γ, are more likely to be lost down the beam pipe. Figure 5 illustrates R_{chrg} plotted in different bins of $|\cos\theta_\gamma|$ for events where the recoil mass is in the range: 4-5 GeV/c^2. The fact that the multiplicity ratio of $gg\gamma$ to $q\bar{q}\gamma$ is uniform in all bins of $|\cos\theta_\gamma|$ indicates that the measured R_{chrg} value is not biased by such acceptance effects.

2. N_{chrg} cut

In order to investigate the sensitivity of the result to the $N_{chrg} \geq 3$ requirement and to suppress $\tau\tau\gamma$ backgrounds, we compare the ratios obtained from $2.5 < N_{chrg}$ with truncated ratios (defined as taking the means from the multiplicity interval $4.5 < N_{chrg} < 11.5$). The difference between the ratio value with a truncated vs. non-truncated mean is found to be 0.0003. This comparison also partially addresses possible biases in our measured ratio due to differences in the true, underlying quark/gluon multiplicity distribution. A complete Monte Carlo simulation study of possible differences between the ratio of detector level multiplicities and the true multiplicities, including unfolding effects, indicates no such bias.

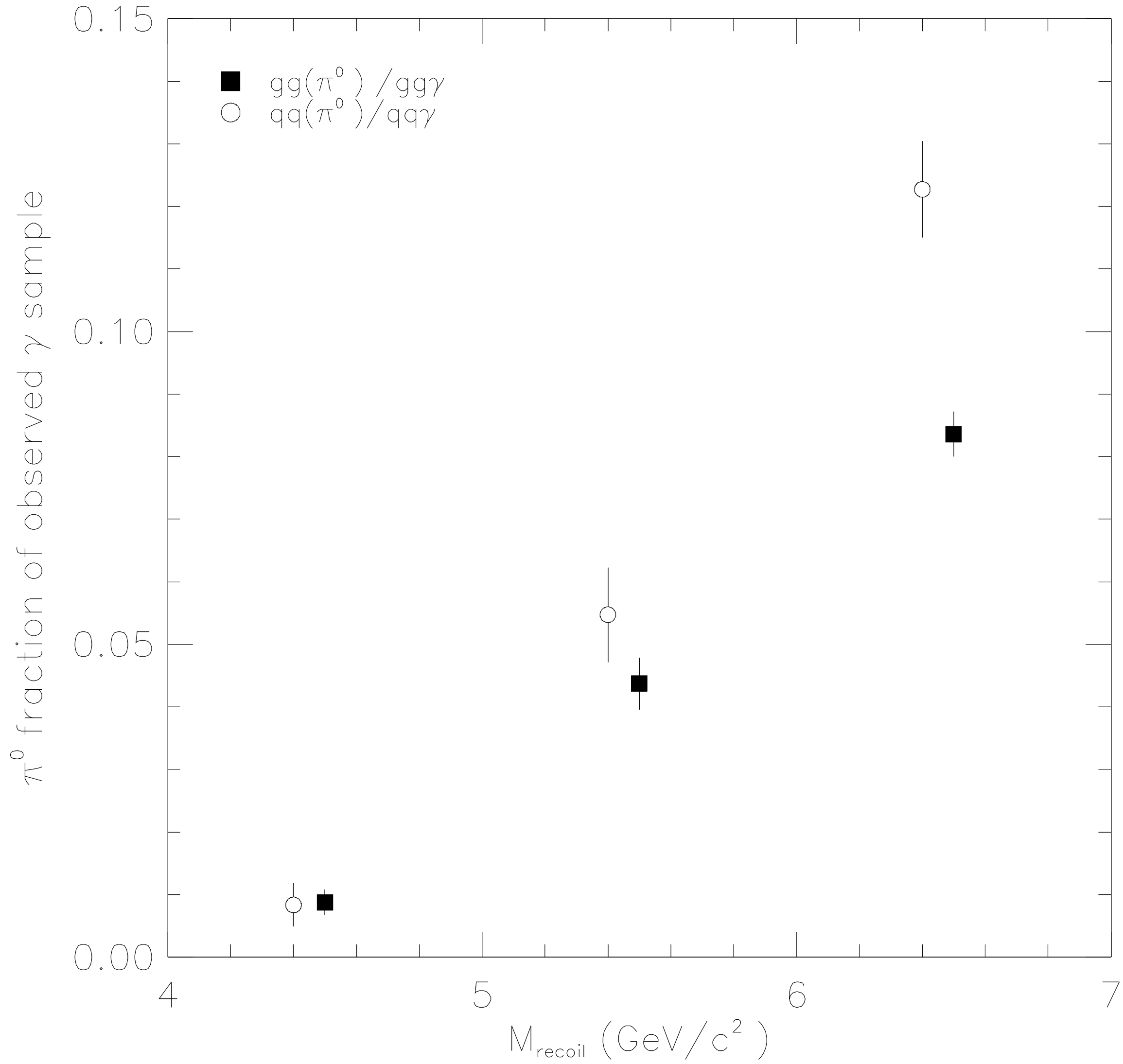

FIG. 1. π^0 contamination, as a function of recoil mass, in $gg\gamma$ events (squares), and in $q\bar{q}\gamma$ events (circles); the y axis gives the fraction of our apparent $gg\gamma$, (or $qq\gamma$), event sample which are actually $gg(\pi^0)$, (or $qq(\pi^0)$), events.

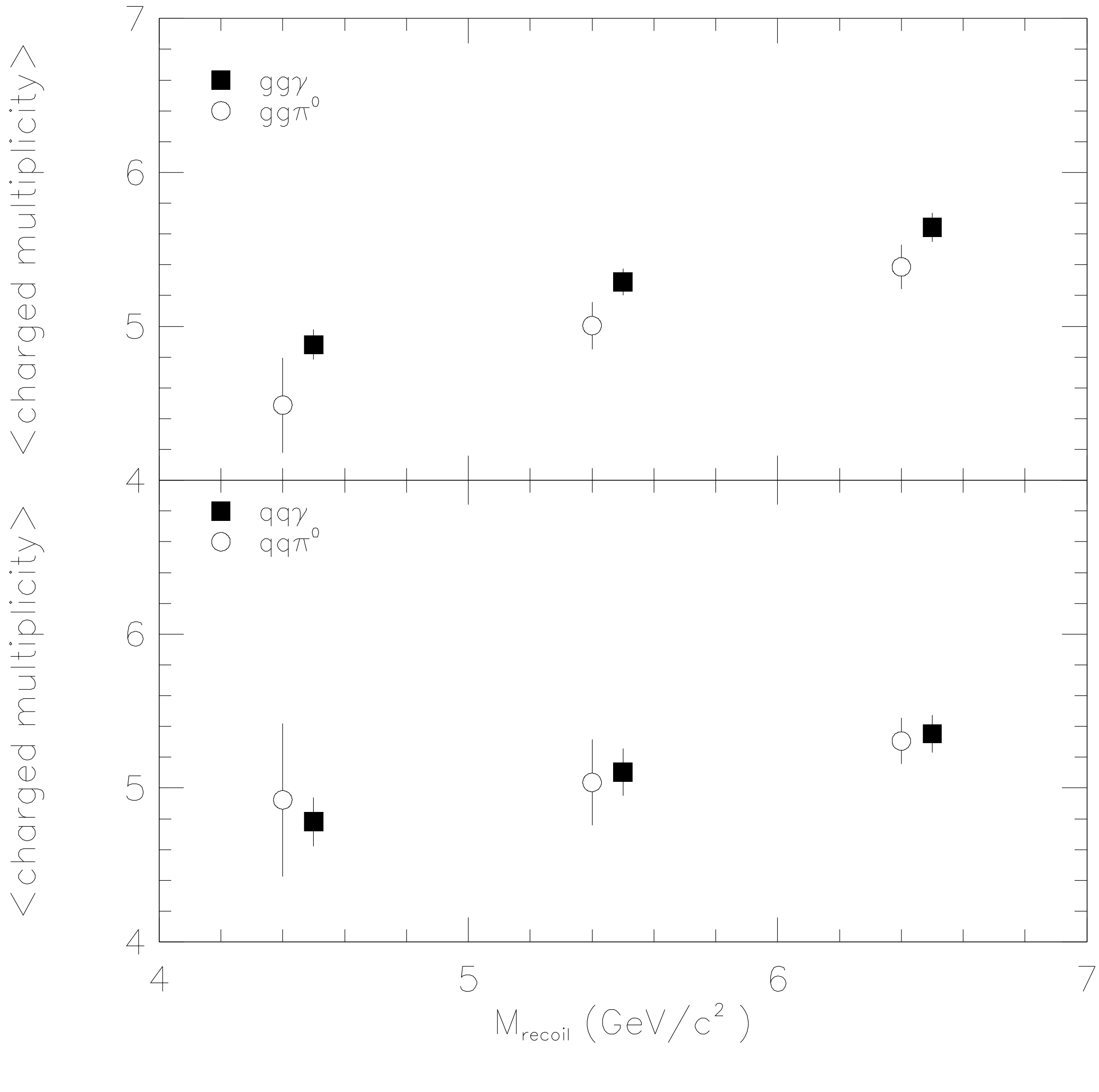

FIG. 2. A comparison of the charged multiplicity distributions for $gg\gamma$ and $ggg(\pi^0)$ (top) and $q\bar{q}\gamma$ and $q\bar{q}(\pi^0)$ (bottom).

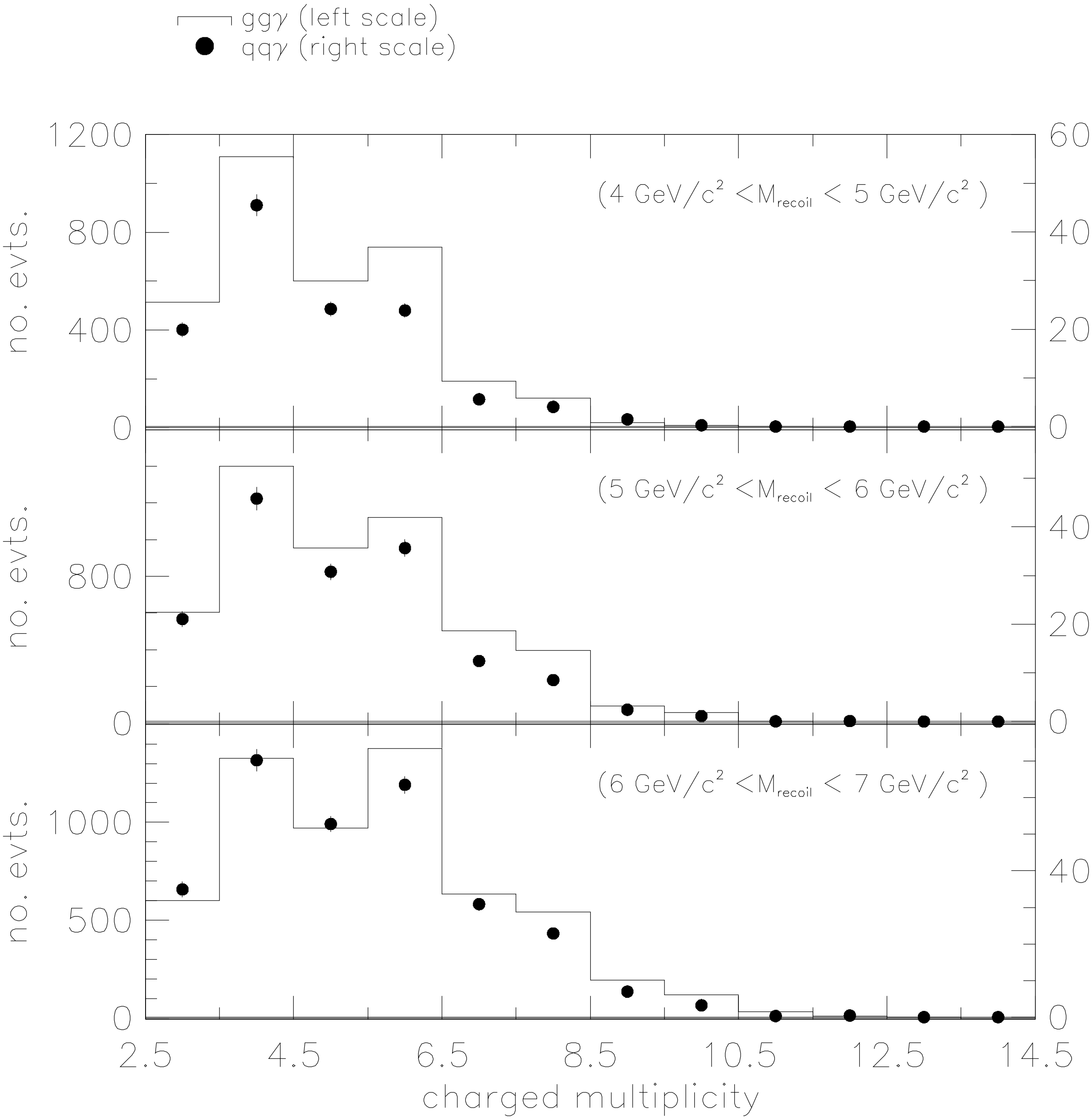

FIG. 3. Observed multiplicity distributions for background subtracted $gg\gamma$ and $q\bar{q}\gamma$ data for slices in recoil mass.

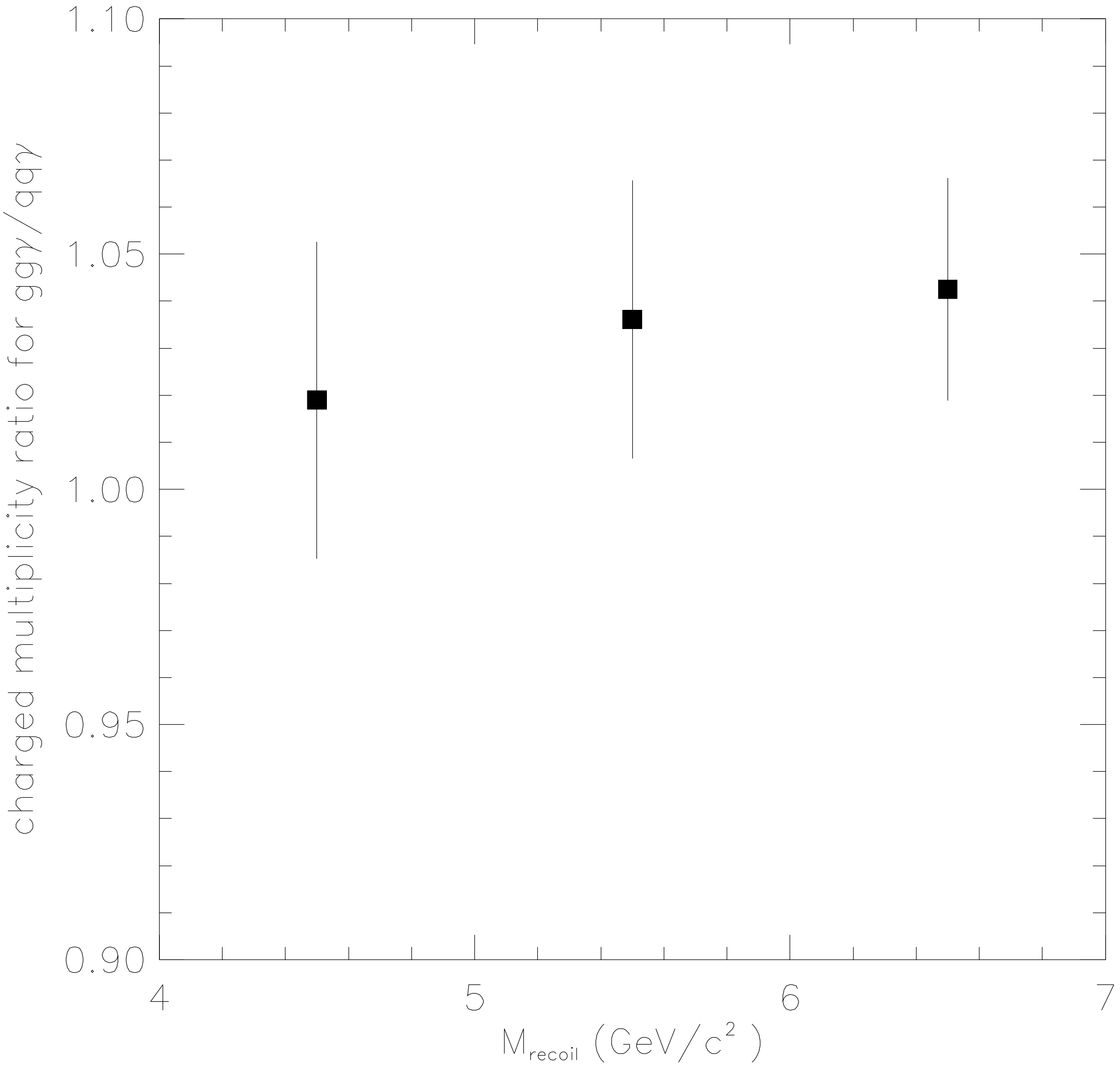

FIG. 4. Charged multiplicity ratio for background subtracted $gg\gamma/q\bar{q}\gamma$ data.

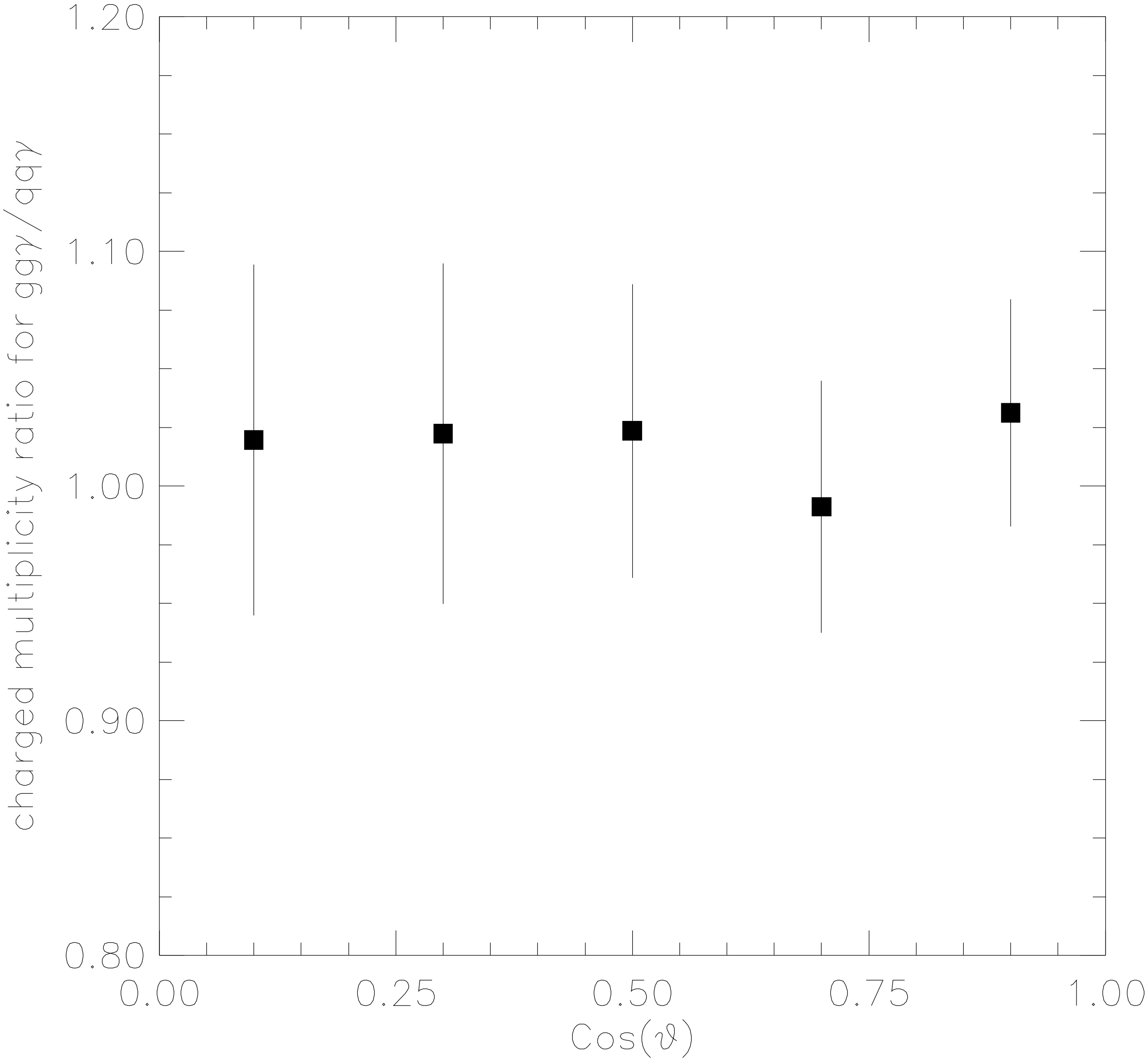

FIG. 5. Plot of $gg\gamma/q\bar{q}\gamma$ multiplicity ratio as a function of $\cos\theta$, with 4 GeV/c^2 < M$_{\rm recoil}$ < 5 GeV/c^2 for background subtracted $gg\gamma$ and $q\bar{q}\gamma$ data.

3. Energy difference effects

Although we compare systems of equivalent mass, the energies of the systems recoiling against the photon are higher for $q\bar{q}$ events than for gg events at an equivalent invariant mass. On average, the $q\bar{q}\gamma$ system will therefore be more collimated. We investigated possible energy dependent effects with Monte Carlo simulation, by looking at systems of equal recoil mass, but different energies. We found a systematic shift of 0.006 in the ratios.

We finally compare the $gg\gamma/q\bar{q}\gamma$ multiplicity ratios from data taken during three distinct running periods, covering different running conditions and triggers. The separate data sets give ratios which are all statistically consistent with each other. Nevertheless, we conservatively include the maximum variation of 3% observed between data sets in the overall systematic error.

In summary:

Systematic Error	Value
π^0 background	0.003
$\lvert\cos\theta\rvert$ cut dependence	0.02
Truncated ($4.5 < N_{chrg} < 11.5$) vs. non-truncated mean	0.02
Variation between data sets	0.03
Recoil effects	0.006
Total	0.04

V. SUMMARY

The ratio of $< N_{chrg} >$ for gluons to $< N_{chrg} >$ for quarks measured here is smaller than those found by the OPAL, ALEPH, SLD and DELPHI experiments, at $\sqrt{s} \sim M_{Z^0}$. The ratios compare as follows:

Collaboration	$< N >_g / < N >_q$	Kinematic Regime
CLEO 96	1.04 ± 0.04	$< E_{jet} > \ < \ 7$ GeV
DELPHI [2]	1.24 ± 0.015	$< E_{jet} > =$ 10-40 GeV
SLD [13]	1.36 ± 0.24	$< E_{jet} > = 24$ GeV
OPAL 93 [15]	1.27 ± 0.04	$< E_{jet} > = 24$ GeV
ALEPH [17]	1.19 ± 0.04	$< E_{jet} > = 24$ GeV
OPAL 96 [18]$*$	1.58 ± 0.03	$< E_{jet} > = 39$ GeV

$*$This OPAL result is for $< N >_g -1/ < N >_q -1$, considering only *uds* quarks

Fuster and Martí [1], DELPHI [2] and Fodor [3] have recently considered how the ratio of charged multiplicity for gluon to quark jets depends on the hadronic center-of-mass energy. As the center-of-mass energy increases, the multiplicity distributions for gluons and quarks diverge, hence their ratio increases with increased energy. Fuster and Martí have looked at the multiplicity results for DELPHI, OPAL, ALEPH and HRS-PEP and have evolved them down to a jet energy as low as 10 GeV. Our result is consistent with the extrapolation of LEP results to $\sqrt{s} = 10$ GeV. We note that the $q\bar{q}$ mixture in this experiment is likely to be different than the quark mixture for the high energy experiments mentioned above. Recent analyses by OPAL [19] and ALEPH [17], in fact, have explicitly measured the difference in ratio values when comparing gluon jets to b-quark jets versus gluon jets to uds-quark jets.

VI. ACKNOWLEDGMENTS

We gratefully acknowledge the effort of the CESR staff in providing us with excellent luminosity and running conditions. J.P.A., J.R.P., and I.P.J.S. thank the NYI program of the NSF, G.E. thanks the Heisenberg Foundation, K.K.G., M.S., H.N.N., T.S., and H.Y. thank the OJI program of the DOE, J.R.P., K.H., and M.S. thank the A.P. Sloan Foundation, L.J.W. thanks the Hughes Foundation, and A.W. and R.W. thank the Alexander von Humboldt Stiftung for support. This work was supported by the U.S. National Science Foundation, the U.S. Department of Energy, and the Natural Sciences and Engineering Research Council of Canada.

REFERENCES

[1] J. Fuster and S. Martí, "Charged Particle Production in the Fragmentation of Quark and Gluon Jets," to appear in the proceedings of the XXXII conference of the European Physics Society, High Energy Physics, Brussels, 27 July- 3 August (1995), HEP-EX/9511002, (1996).

[2] P. Abreu et al. (DELPHI Collaboration), CERN-PPE/95-164 "Energy Dependence of the Differences between the Quark and Gluon Jet Fragmentation," to be submitted to *Zeit f. Physik C.*, (1995).

[3] Z. Fodor, "Differences between quark and gluon jets at LEP," *Physics Letters*, *B263*, p. 305, (1991).

[4] S. Bethke "JADE Results on Quark and Gluon Fragmentation," *Zeit f. Physik C. (Particles and Fields)*, *29*, p. 175, (1985).

[5] F.H. Heimlich (CRYSTAL BALL Collaboration), "Gluon and Quark Fragmentation in the Upsilon Region," in the Heidelberg 1986, Proceedings, Production and Decay Of Heavy Hadrons, 76-80, (1986).

[6] D. H. Saxon, RAL-86-057 "Quark and Gluon Fragmentation in High-Energy E+ E- Annihilation," based on lectures given at the International School of High Energy Physics, Duilovo-Split, Yugoslavia, Sep 21 - Oct 5, 1986, in Ali, A. (ED.), Soeding, P. (ED.): High Energy Electron-Positron Physics 539-610 and Chilton Rutherford Lab. - RAL-86-057 (86,REC.SEP.) 62p, (1986).

[7] G. Arnison et al. (UA1 Collaboration), "Analysis of the Fragmentation Properties of Quark and Gluon Jets at the CERN SPS P Anti-P Collider," *Nuclear Physics*, *B276*, p. 253, (1986).

[8] R. Waldi (ARGUS Collaboration), "Recent Results from ARGUS on Quark and Gluon Fragmentation in the Upsilon Energy Region," in LUND 1984 Proceedings, Multiparticle Dynamics 808-817 and Heidelberg Univ. IHEP-HD 84-07 (84, REC.SEP.), (1984).

[9] G. C. Moneti HEPSY 6-84 "Gluon Versus Quark Fragmentation," *Lund Multipart.Dyn.*, 1984:782 *QCD161:C49*, (1984).

[10] Paul Hoyer, "Model Independent Analysis of Quark and Gluon Fragmentation," *Physics Letters*, *B133*, p.108, (1983).

[11] J. William Gary, "On the Multiplicity difference between Quark and Gluon Jets," *Physical Review D 49*, p. 4503, (1994).

[12] E. D. Malaza and B. R. Webber, "Multiplicity Distributions in Quark and Gluon Jets," *Nuclear Physics B 267*, p. 702, (1986).

[13] Yoshihito Iwasaki (SLD Collaboration), "A Measurement of Quark and Gluon Jet Differences at the Z^0 Resonance," SLAC-R-95-460, (1995).

[14] G. Alexander et al. (OPAL Collaboration), "A Direct Observation of Quark-Gluon Jet Differences at LEP," *Physics Letters B265*, p. 462, (1991).

[15] R. Akers (OPAL Collaboration), "A Study of Differences Between Quark and Gluon Jets Using Vertex Tagging of Quark Jets," CERN-PPE/95-075 sub. to Zeit. for Phys. C, (1993).

[16] R. Akers et al. (OPAL Collaboration), "A Model Independent Measurement of Quark and Gluon Jet Properties and Differences," *Zeit. for Phys. C*, *68*, p. 179, (1995).

[17] D. Buskulic et al. (ALEPH Collaboration) " Quark and Gluon Jet Properties in Symmetric Three Jet Events," CERN-PPE-95-184, subm. to *Phys. Lett.*, (1995).

[18] Wojtek Bogusz et al. (OPAL Collaboration), Physics Note PN218 "Test of QCD analytic predictions for the mean multiplicity difference between gluon and quark jets", submitted to

the 1996 APS Meeting of the Division of Particles and Fields, Minneapolis, MN (1996).

[19] G. Alexander et al. (OPAL Collaboration), "Comparison of b & uds quark jets to gluon jets," *Zeit. for Phys. C 69*, p. 543, (1995).

[20] Y. Kubota *et al*, CLEO Collab., "The CLEO-II detector", Nucl. Instr. Meth. **A320**, 66 (1992).